JOURNAL OF GUIDANCE, CONTROL, AND DYNAMICS
Vol. 16, No. 2, March-April 1993

Attitude Dynamics and Control of a Vertical Interferometric Radar Tethered Altimeter

A. Moccia,* S. Vetrella,* and M. Grassi†
University of Naples, Naples, 80125 Italy

This paper investigates the attitude dynamics and control of a vertical interferometric synthetic aperture radar tethered altimeter: a system based on two space platforms of comparable mass connected by 1-km tether. Two vertically spaced physical antennas on these platforms supply the terrain height measurement data by making use of radar interferometry. Since the height accuracy is strongly affected by the combined dynamics of the two platforms, this paper will focus on the analysis and control of high-frequency attitude oscillations. The results show that the proposed control system can limit the attitude angle differences and rates to 10^{-3} and 10^{-4} deg/s, respectively, as required by the proposed application.

Nomenclature

a	= MS orbit semimajor axis
B	= interferometric baseline
h	= height
h_w	= modulus of the reaction wheel angular momentum
I_1, I_2, I_3	= inertia principal moments of the platform
I_w	= inertia moment of the reaction wheel
K_a	= microwave spectral band, 35 GHz
$k_\alpha, k_\beta, k_\gamma$	= roll, pitch, and yaw gains
l_i	= stretched length of the ith tether segment
$M_{d1}\ M_{d2}\ M_{d3}$	= aerodynamic torque components with respect to the principal reference frame
R	= MS slant range
r_e	= local Earth radius
r_1, r_2, r_3	= attachment point coordinates with respect to the principal reference frame
T_{ij}	= modulus of the tether tension between the ith and jth lumped masses
x, y, z	= orbiting reference frame
1,2,3	= principal reference frame
α, β, γ	= roll, pitch, and yaw angles
$\Delta\varphi$	= interferometric phase difference
ϵ_1, ϵ_2	= in-plane and out-of-plane tether lateral deflections
ζ	= damping factor
θ	= off-nadir viewing angle
λ	= wavelength
σ_h	= height measurement uncertainty
$\sigma_\alpha, \sigma_\beta, \sigma_\gamma$	= roll, pitch, and yaw measurement uncertainties
$\tau_\alpha, \tau_\beta, \tau_\gamma$	= roll, pitch, and yaw time constants
Ω	= orbital angular velocity

Subscripts

fv	= final value
mv	= maximum value

Introduction

SEVERAL scientific and technological missions have been proposed using different space platforms connected by cables,[1,2] including a joint U.S.-Italian program aimed at deploying a small satellite (tethered satellite system) from the Shuttle during two demonstration flights.[3]

The tethered system's orbital dynamics have been studied by several authors, who considered different space configurations during deployment, stationkeeping, and retrieval. Nevertheless, the dynamical behavior of tethered systems still needs further investigation, in particular when an accurate position and attitude control are required.

A spaceborne remote sensing mission, in which two vertically spaced physical antennas are carried along parallel paths by two platforms connected by a short tether, has been proposed in Ref. 4. The antenna on the mother satellite (MS) transmits radar signals, and both antennas receive return signals. The output of the synthetic antennas is combined to form an interferometric synthetic aperture radar (SAR). The high-resolution image of the Earth's surface is provided by SAR technology, and the terrain height measurement is carried out by radar interferometry, because of the distance between the antennas (baseline).[5]

Among the different proposed space remote sensing missions, SAR interferometry is considered one of the most promising techniques for global topographic mapping.[6] In addition to tethered SAR interferometry, two other proposed techniques are worth mentioning: a rigid boom connecting the two antennas and multiple-orbits interferometry. A short horizontal baseline (10 m) has been proposed, considering a single spacecraft with the two antennas mounted on a rigid boom.[7] Since practical considerations limit the length of the boom, it is necessary to use a shorter wavelength (K_a band), which implies significant drawbacks: an increased sensor complexity, difficulty in achieving electronic steering of the antenna and, consequently, less frequent observations, a greater atmospheric effect, limited experience in the application of these short wavelengths, and high-frequency structural vibrations with an amplitude comparable to the wavelength. However, a longer baseline can be obtained when a single antenna observes the same area from two different orbits separated in a cross-track direction.[8] This technique presents significant advantages at a relatively low cost, but several aspects make its operational use unlikely: baseline indetermination and variation, no simultaneous images, strong decorrelation due to changes in the backscatter characteristics of the terrain, and difficulty in selecting the orbit for an adequate coverage.

On the other hand, a tethered interferometer presents several advantages over these latter solutions. In particular, by using this technique, a better angular accuracy can be obtained by increasing the baseline, and height measurement by combining two simultaneous images becomes possible. Moreover, various new experiments using a long and variable baseline can be carried out, while still incorporating already proven SAR technology.[9,10] Finally, tethered interferometry takes advan-

Received July 15, 1991; revision received March 2, 1992; accepted for publication March 25, 1992.

*Chair, Aerospace Systems Engineering, Faculty of Engineering, P.le Tecchio 80.

†Ph.D. Student, Aerospace Engineering, P.le Tecchio 80.

tage of the already envisaged investments and improvements in tether technology; since the tether can be used as a power and/or communication line, it is therefore possible to simplify the design of the two spacecrafts. On the other hand, the high-frequency oscillations of the tethered system affect the accuracy of the phase difference measurement between the two SAR images and, therefore, the height measurement error.

In-plane, out-of-plane, and longitudinal low-frequency oscillations of the order of the orbital rate cause variations in the distance between the antennas that can be measured by laser sensors within adequate accuracy.[11]

As far as the high-frequency longitudinal oscillations are concerned, an appropriate orbit selection can reduce thermal effects on the tether, and hence the amplitude of the oscillations can be made practically negligible. Moreover, several authors have shown that adequate control laws can effectively damp high-frequency longitudinal oscillations.[12-14]

Hence, this paper deals with the attitude dynamics and control of two space platforms of comparable mass that are connected by a 1-km tether. This length has been chosen as a tradeoff among the achievable height accuracy,[4-10] the baseline decorrelation effect,[5] and the increase of the gravity gradient.

Conventional torquing actuators[15-17] or more specific techniques, such as the tether attachment point motion,[18,19] have been proposed for the attitude control of tethered systems. In particular, in Ref. 15 a mathematical model is developed for the control of a tethered platform subsatellite system by modulating the tension level in the tether with momentum-type platform-mounted devices. In Ref. 16, the dynamical behavior of two space platforms connected by a short tether is analyzed, with special emphasis on the attitude dynamics of the subsatellite: two fins are designed to stabilize it around the yaw axis. In Ref. 17, results of the dynamics simulation performed for the attitude measurement and control subsystem for the first tethered satellite system (TSS) mission are shown. Side thrusters are used to control in-plane and out-of-plane librations of the system and the yaw dynamics of the satellite; the roll and pitch axes are stabilized by gravity gradient effects. Finally, in Refs. 18 and 19, a new attitude control technique based on the attachment point motion to produce torque about the pitch and roll axes is presented.

In this paper we propose an attitude control law based on the motion of the tether attachment point to damp pitch and roll high-frequency oscillations and based on a reaction wheel to reduce the yaw angle difference between the two platforms. The gains and time constants of the control law are derived from a simplified analytical model, and then the orbital and attitude dynamics are studied by using a computer simulation.[20]

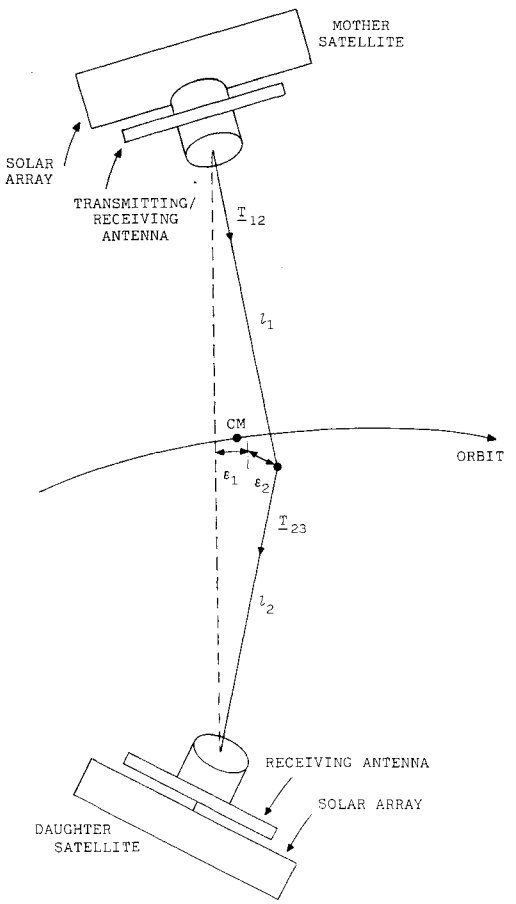

Fig. 1 Schematic of the vertical interferometric SAR tethered altimeter.

System Configuration

With reference to Fig. 1, each platform is assumed to be a rigid body, approximated by simple geometrical elements. In particular, two rectangular flat plates, representing the antenna and the solar array, are connected to a main cylindrical module, so that the aerodynamic torques are balanced.

The tether is represented by a single lumped mass connected to the platforms by massless spring dashpots meant to simulate longitudinal and stringlike vibrations.

The platforms and the tether characteristics are shown in Tables 1 and 2, respectively.

A sun-synchronous orbit, at an altitude of 450 km, has been selected. To reduce longitudinal oscillations due to thermal effects and to simplify the solar panel orientation, the ascending node is at 6 p.m. local time.[21]

The attitude dynamics are described considering the yaw, pitch, and roll attitude angles as the Euler angles of the principal axes of each platform, with respect to the same right-handed reference frame (whose origin is at the center of mass of the mother satellite, the z axis is coincident with its position vector and directed downward, the y axis is perpendicular to the orbital plane, and the x axis is directed forward; see Fig. 2).

Analytical Model

The attitude analytical model is based on the following assumptions: the platform center of mass is in Keplerian circular orbit, the tether is represented by one lumped mass, the gravitational potential is linearized, small perturbations are assumed, the tether attachment point is initially set on the verti-

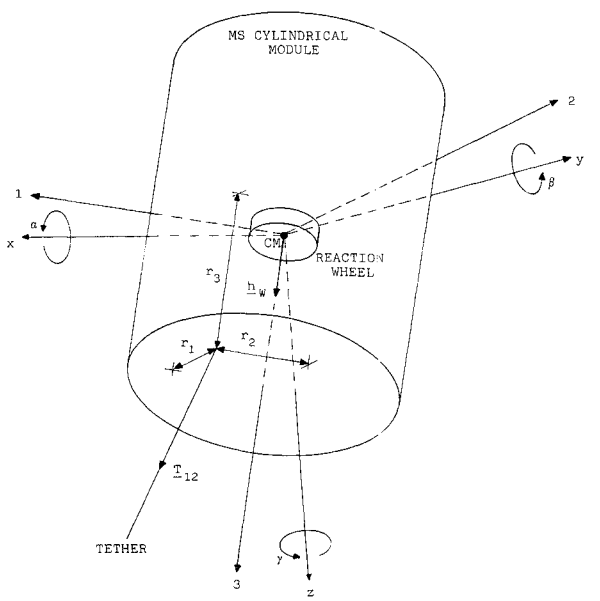

Fig. 2 Schematic of the mother satellite attitude reference frames and the control technique.

Table 1 Platform characteristics

		Cylindrical module		Flat plates		Inertia principal moments			Attachment point coordinates		
Platform	Mass, kg	Radius, m	Height, m	Antenna area, m^2	Solar array area, m^2	I_1, kg m^2	I_2, kg m^2	I_3, kg m^2	r_1, m	r_2, m	r_3, m
MS	1400	0.90	2	22.62	24	2780.11	4028.09	5212.55	0	0	1.19
DS	800	0.50	1	22.62	12	625.22	2728.24	2828.69	0	0	−0.68

Table 2 Tether characteristics

Radius	5.0×10^{-3} m
Linear density	8.95×10^{-2} kg/m
Sun radiation absorptivity	0.5
Thermal emissivity	0.75
Specific heat	2.5×10^{3} J kg^{-1} K^{-1}
Young's modulus	1.95×10^{10} Nm^{-2}
Thermal expansion coefficient	-6.1×10^{-6} K^{-1}
Damping coefficient	0.05
Drag coefficient	2.0

Table 3 System eigenfrequencies

	MS		DS	
DOF	Frequency, Hz	Period, s	Frequency, Hz	Period, s
Roll	4.62×10^{-3}	216.40	7.31×10^{-3}	136.80
Pitch	3.83×10^{-3}	260.90	3.49×10^{-3}	286.50
Yaw	8.72×10^{-5}	11,470	1.54×10^{-4}	6502

Table 4 System eigenvectors normalized modules

	MS			DS		
Mode	Roll	Pitch	Yaw	Roll	Pitch	Yaw
1	1	0	2.9×10^{-2}	1	0	6.3×10^{-1}
2	0	1	0	0	1	0
3	1.0×10^{-3}	0	1	6.0×10^{-4}	0	1

cal principal axis, and the tether longitudinal dynamics and control and thermal effects are assumed negligible. Consequently, the MS attitude equations are

$$\ddot{\alpha}+4a\Omega^2\alpha-(1-a)\Omega\dot{\gamma}=-\left(\frac{r_3T_{12}}{I_1}\right)\alpha-\left(\frac{r_3T_{12}}{I_1l_1}\right)\epsilon_2+\frac{M_{d1}}{I_1}$$

$$\ddot{\beta}+3\Omega^2c\beta=\left(\frac{r_3T_{12}}{I_2}\right)\beta+\left(\frac{r_3T_{12}}{I_2l_1}\right)\epsilon_1+\frac{M_{d2}}{I_2}$$

$$\ddot{\gamma}+b\Omega^2\gamma+(1-b)\Omega\dot{\alpha}=\frac{M_{d3}}{I_3} \tag{1}$$

where

$$a=\frac{(I_2-I_3)}{I_1}$$

$$b=\frac{(I_2-I_1)}{I_3}$$

$$c=\frac{(I_1-I_3)}{I_2} \tag{2}$$

The modulus of the tension in the upper tether segment is computed considering the spring dashpot model and the gravity gradient. In the same way, it is possible to obtain the attitude equations of the daughter satellite (DS), which will be omitted in this paper for the sake of brevity.

Extending the Lemke et al.[18] formulation, the torques due to the tether tension and the aerodynamics have been introduced as a function of the pitch and roll angles, both in-plane and out-of-plane tether stringlike vibrations, and aerodynamic forces. The tether vibrations and the aerodynamic torques have been modeled with periodic functions, whose parameters have been computed by making use of simplified models and numerical simulation.

The eigenfrequencies and the normalized eigenvector modules are shown in Tables 3 and 4, respectively. In spite of the tether, the pitch dynamics is decoupled, whereas the roll and yaw angles are weakly coupled because of the orbital dynamics. Equations (1) show that the yaw eigenfrequency is determined by the gravity gradient, whereas the pitch and roll amplitudes are limited by the tether restoring forces.[16,18,22]

Attitude Control

The attitude control is based on moving the tether attachment point on a flat surface to produce control torques for pitch and roll high-frequency damping.[18,19] This technique leads to large yaw errors in the presence of steady-state disturbances, and/or to an excessive roll amplification.[18] Consequently, yaw control is obtained by using a reaction wheel with the spin axis directed along the platform yaw axis.

By introducing in Eqs. (1) the attachment point motion and the reaction wheel angular momentum, we get

$$\ddot{\alpha}+\left[\left(4a-\frac{I_w}{I_1}\right)\Omega^2+\frac{r_3T_{12}}{I_1}\right]\alpha-\left[(1-a)+\frac{I_w}{I_1}\right]\Omega\dot{\gamma}$$

$$+\frac{h_w}{I_1}(\dot{\beta}-\Omega)=\frac{r_2T_{12}}{I_1}-\left(\frac{r_3T_{12}}{I_1l_1}\right)\epsilon_2+\frac{M_{d1}}{I_1}$$

$$\ddot{\beta}+\left(3c\Omega^2+\frac{r_3T_{12}}{I_2}\right)\beta+(\Omega\gamma-\dot{\alpha})\frac{h_w}{I_2}=-\frac{r_1T_{12}}{I_2}$$

$$+\left(\frac{r_3T_{12}}{I_2l_1}\right)\epsilon_1+\frac{M_{d2}}{I_2}$$

$$\left(1+\frac{I_w}{I_3}\right)\ddot{\gamma}+b\Omega^2\gamma+\left[(1-b)+\frac{I_w}{I_3}\right]\Omega\dot{\alpha}-\left(\frac{r_1T_{12}}{I_3}\right)\alpha$$

$$-\left(\frac{r_2T_{12}}{I_3}\right)\beta+\frac{\dot{h}_w}{I_3}=\left(\frac{r_1T_{12}}{I_3l_1}\right)\epsilon_2-\left(\frac{r_2T_{12}}{I_3l_1}\right)\epsilon_1+\frac{M_{d3}}{I_3} \tag{3}$$

Since the system described by Eqs. (1) is controllable and observable, and if we neglect the roll-yaw coupling, it is possible to introduce three independent control laws as follows:

$$r_2=k_\alpha(\alpha+\tau_\alpha\dot{\alpha})$$

$$r_1=k_\beta(\beta+\tau_\beta\dot{\beta})$$

$$\dot{h}_w=k_\gamma(\gamma+\tau_\gamma\dot{\gamma}) \tag{4}$$

where

$$k_\alpha = r_3\left(1-\frac{\epsilon_{2mv}}{I_1\alpha_{fv}}\right)+4a\Omega^2\frac{I_1}{T_{12}}$$

$$\tau_\alpha = -\frac{2I_1}{T_{12}k_\alpha}\left[(r_3-k_\alpha)\frac{T_{12}}{I_1}+4a\Omega^2\right]^{1/2}\zeta$$

$$k_\beta = r_3\left(\frac{\epsilon_{1mv}}{I_1\beta_{fv}}-1\right)-3c\Omega^2\frac{I_2}{T_{12}}$$

$$\tau_\beta = \frac{2I_2}{T_{12}k_\beta}\left[(r_3+k_\beta)\frac{T_{12}}{I_2}+3c\Omega^2\right]^{1/2}\zeta$$

$$k_\gamma = I_3\left(\frac{M_{d3mv}}{I_3\gamma_{fv}}-b\Omega^2\right)$$

$$\tau_\gamma = \frac{2I_3}{k_\gamma}\left(b\Omega^2+\frac{k_\gamma}{I_3}\right)^{1/2}\zeta \qquad (5)$$

The numerical values are computed assuming a unit damping coefficient and 10^{-3} degrees as steady-state error for the attitude angles (Table 5). The latter value has been derived by considering the maximum height error due to the misalignment of the two antennas. Assuming uncorrelated parameters, the height measurement uncertainty due to such misalignment is given by:

$$\sigma_h^2 = \left(\frac{\partial h}{\partial\alpha}\right)^2\sigma_\alpha^2+\left(\frac{\partial h}{\partial\beta}\right)^2\sigma_\beta^2+\left(\frac{\partial h}{\partial\gamma}\right)^2\sigma_\gamma^2 \qquad (6)$$

where the height of each resolution element above a local spherical Earth is computed as follows[10]:

$$h = \left[(a-R\cos\theta)^2+(R\sin\theta)^2\right]^{1/2}-r_e \qquad (7)$$

For the sake of brevity we will focus our attention only on the effects of the pitch angle difference because pitch uncertainty is the major contribution to the height error. With reference to Fig. 3 and for small pitch angles, we obtain

$$\frac{\partial h}{\partial\beta} \cong (2R-B\cos\theta)(R\cos\theta-B)\frac{a\tan\psi}{Br_e} \qquad (8)$$

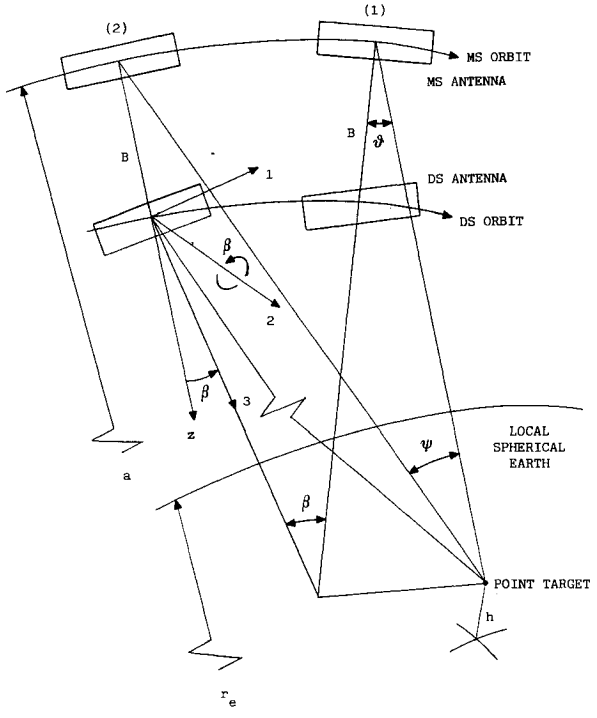

Fig. 3 Effect of a pitch angle difference on the interferometric phase difference.

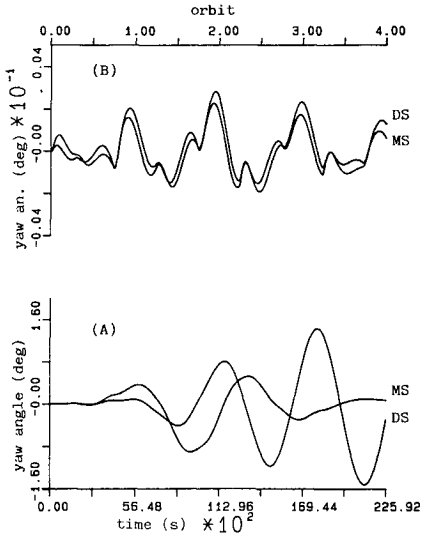

Fig. 4 Yaw angle of the mother and daughter satellites a) without control and b) with control.

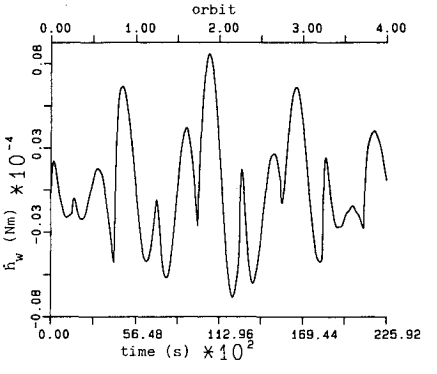

Fig. 5 Control torque of the reaction wheel on board the mother satellite.

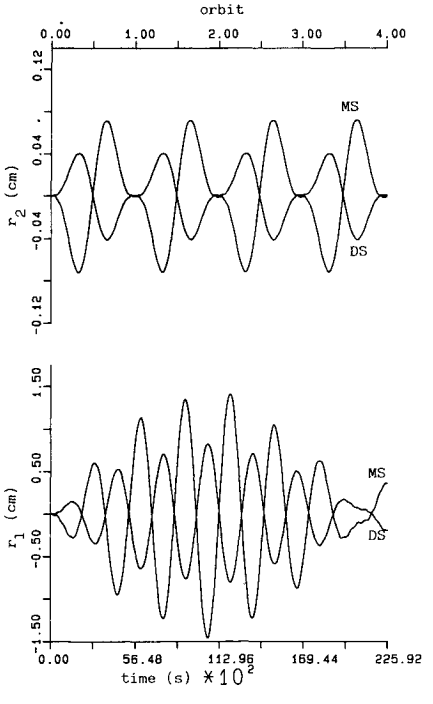

Fig. 6 Tether attachment point displacements along the principal axes (1, 2) of the mother and daughter satellites.

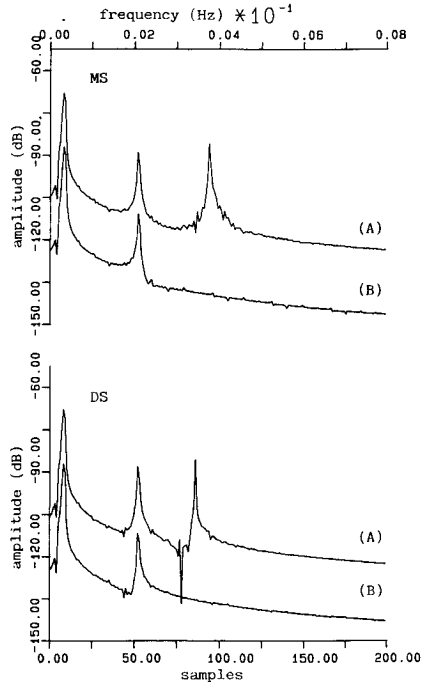

Fig. 7 Spectra of the pitch rate of the mother and daughter satellites a) without control and b) with control.

where

$$\tan\psi = \left(\frac{R\cos\theta - B}{R}\right)\tan\beta \tag{9}$$

Equation (8) has been derived by considering the interferometric phase difference between the orbital position of Eq. (1), where the point scatterer is in the plane perpendicular to the MS antenna, and the orbital position of Eq. (2), where the point scatterer is in the plane perpendicular to the DS antenna:

$$\Delta\varphi = \left(\frac{2\pi}{\lambda}\right)\left[\frac{B\cos\theta - 2R(1-\cos\psi)}{\cos\psi}\right] \tag{10}$$

As a consequence, the point scatterer is not focused simultaneously by the two antennas and this will affect the height measurement accuracy, depending on the antenna's attitude difference and its accuracy. Considering that the proposed tethered interferometric altimeter also has real-time applications (i.e., natural disasters monitoring and mapping), it is necessary to limit the height uncertainty (to the order of 1 m), so as to avoid significant and time-consuming Earth-based post-processing, which is normally applied for low-frequency phenomena. By repeating the previous analysis for the roll and yaw differences and using Eq. (6), we obtain 10^{-3} deg as an adequate maximum value for the differences in antenna attitude angles.

Numerical Simulation

A three-dimensional numerical model, based on the discretization of the system by means of lumped masses, connected by massless springs and dashpots,[16-20] has been improved to test the attitude control law, which had been derived using the analytical model. The system orbital motion is described by the force and energy balance differential equations, the unknown quantities being the temperature and the components of the position and velocity vectors in the right-handed inertial reference frame (whose origin is at the center of the Earth, the X-axis is directed along the first point of Aries, and the X-Y plane coincides with the equatorial one).

The environmental perturbations considered are the force of gravity, including the second zonal harmonic of the gravity field, the aerodynamic forces, and the thermal effects on the tensional forces. The two end masses represent the mother and daughter satellites; the intermediate mass (the mass is 44.75 kg, the area is 5 m^2) simulates the tether.

The platform attitude is simulated by means of the kinematics and the Euler moment differential equations, the unknown quantities being the Euler angles of the body reference frame (whose axes coincide with the principal axes) with respect to the inertial reference frame and the body components of the angular velocity vector. The roll, pitch, and yaw angles of each platform are derived by using transformation matrices. The torques are computed by taking into account the aerodynamic drag, the tether visco-elastic force, the gravity gradient, and the attitude control. The total aerodynamic torque is computed by adding the contribution of each geometrical element, which approximates the platform, and by neglecting the spin effect.

The system orbital and attitude dynamics are computed by solving a set of ordinary differential first-order equations.

The simulation starts with the system at the ascending node on the X axis of the inertial reference frame, aligned along the local vertical and at zero attitude angles. The tether temperature shows small oscillations centered about 267 K, when the simulation is performed during the vernal equinox, due to the selected terminator orbit. Consequently, the high-frequency longitudinal dynamics exhibit negligible amplitudes (of the order of 10^{-5} m) with respect to the requested accuracy in height, so that the tether length control can be dispensed with.

Figure 4 shows the yaw angles before and after the control, and Fig. 5 shows the torque of the reaction wheel on board the mother satellite. The yaw dynamics, which depend mainly on the chosen platform's configurations, can be controlled to the required values by using small reaction wheels.

A small displacement of the tether attachment point (Fig. 6) allows the high-frequency oscillations to be damped and the amplitudes of low-frequency ones to be reduced, as shown by the pitch and roll time derivative spectra plotted in Figs. 7 and 8. In addition, the amplitudes of the discrete-time Fourier transform coefficients show both the system eigenfrequencies, computed also by the analytical model (Table 3), and the disturbing torques' frequencies.[16,22-24]

The maximum values of the differences in attitude angles, between the mother and the daughter satellites, and of the

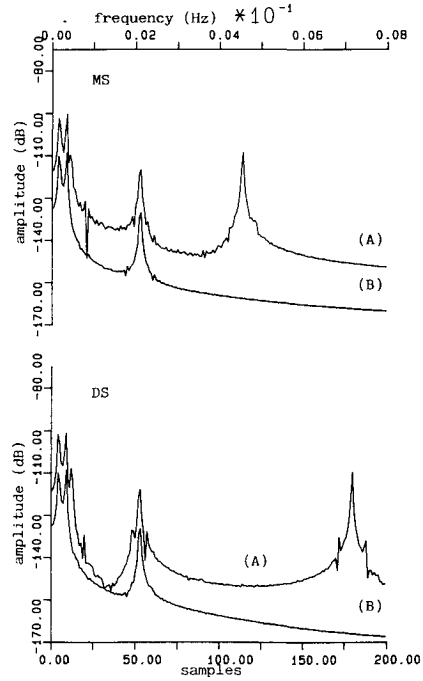

Fig. 8 Spectra of the roll rate of the mother and daughter satellites a) without control and b) with control.

Table 5 Control law gains

Gain	MS	DS
k_α, m	−4.26	2.42
τ_α, s	41.11	26.00
k_β, m	9.70	−6.87
τ_β, s	30.72	30.00
k_γ, Nm	0.20	0.06
τ_γ, s	337.30	444.37

Table 6 Maximum values of the angle differences and rates for the attitude dynamics without and with control

	Without control		With control	
	Difference, deg	Rate, deg/s	Difference, deg	Rate, deg/s
Yaw	2	$2.\times10^{-3}$	$5.\times10^{-4}$	$5.\times10^{-6}$
Pitch	$3.\times10^{-2}$	$2.\times10^{-3}$	$1.\times10^{-3}$	$2.\times10^{-4}$
Roll	$1.\times10^{-2}$	$1.\times10^{-4}$	$1.\times10^{-2}$	$2.\times10^{-5}$

attitude rates, before and after the application of the control torques, are summarized in Table 6. It is worth noting that, without the system control, the pitch difference causes an unacceptable height measurement error [Eqs. (6-8)], and the yaw difference, which is of the order of the 3 dB antenna aperture, can significantly degrade the return signal. The required 10^{-3} deg as the maximum angular difference between the two antennas can be obtained with the control law.

Conclusions

A three-axis attitude control system was presented to limit the height measurement error achievable by a synthetic aperture radar interferometer based on two tethered spacecraft carrying two antennas along parallel paths. The control system integrated a reaction wheel and a mobile tether attachment point on board each platform. To obtain high-resolution global topographic mapping, a control law was developed to limit the antennas' misalignment and to damp high-frequency attitude oscillations. The numerical simulation showed that such a control can be achieved by using a conventional reaction wheel (maximum torque of the order of 10^{-5} Nm) and by slightly moving the tether attachment point (maximum displacement of the order of 1.5 cm).

Future research activities will include 1) a further analysis of the system dynamics by introducing different perturbations, such as shadow cone crossing, and/or the sudden breakdown of the mobile attachment point system; 2) a more comprehensive tether description, due to its significant effect on the dynamical behavior of the system; and 3) a comparative study of different additional actuators, which allow for finer control, not only during stationkeeping, but also during deployment, retrieval, and orbital maneuvering.

Acknowledgments

The work in this paper was carried out with financial contributions from the Italian Ministry for University and Research and the Italian Space Agency.

References

[1]Colombo, G., et al., "Shuttle-Borne Skyhook, A New Tool for Low-Orbital-Altitude Research," Sao Rept., Smithsonian Astrophysics Observatory, Cambridge, MA, Sept. 1974.

[2]Penzo, P. A., and Amman, P. W. (eds.), *Tethers in Space Handbook,* 2nd ed., NASA, Office of Space Flight, Washington, DC, 1989.

[3]Anon., "Tethers in Space Toward Flight," *Proceedings of the Third International Conference on Tethers in Space* (San Francisco, CA), CP892, AIAA, Washington, DC, May 1989.

[4]Moccia, A., and Vetrella, S., "Preliminary Analysis of a SAR Interferometer Using a Tethered System," *American Astronomical Society (AAS) Advances in the Astronautical Sciences,* Univelt, San Diego, CA, Vol. 62, 1987, pp. 607-617.

[5]Li, F. K., and Goldstein, R. M., "Studies of Multibaseline Spaceborne Interferometric Synthetic Aperture Radars," *IEEE Transactions on Geosciences and Remote Sensing,* Vol. 28, No. 1, 1990, pp. 88-97.

[6]Topographic Science Working Group, "Topographic Science Working Group Report to the Land Process Branch, Earth Science and Applications Division, NASA Headquarters," Lunar and Planetary Inst., Houston, TX, 1988.

[7]Rodriguez, E., "An Earth Explorer Global Topography Mission, Strawman Instrument Design Overview," Jet Propulsion Lab./Agenzie Spaziale Italiana Joint Technical Meeting, Pasadena, CA, Jan. 1990.

[8]Gabriel, A. K., and Goldstein, R. M., "Crossed Orbit Interferometry: Theory and Experimental Results from SIR-B," *International Journal of Remote Sensing,* Vol. 9, No. 5, 1988, pp. 857-872.

[9]Angino, G., Moccia, A., Rubertone, F. S., and Vetrella, S., "Interferometric Method for Radar Altimetry," *Proceedings of the Consultative Meeting on Imaging Altimeters Requirements and Techniques,* Mullard Space Science Lab., London, England, UK, 1990 (Paper III.8).

[10]Moccia, A., and Vetrella, S., "A Tethered Interferometric Synthetic Aperature Radar (SAR) for a Topographic Mission," *IEEE Transactions on Geoscience and Remote Sensing,* Vol. 30, No. 1, 1992, pp. 103-108.

[11]Nerheim, N., "Conceptual Design of an Antenna Position Sensor for the GLAM-VISTA (Global Topography Mission-Vertical Interferometric SAR Tethered Altimeter) Mission," Jet Propulsion Lab., Interoffice Memorandum 343-90-283, Pasadena, CA, April 1990.

[12]Lorenzini, E. C., "A Three-Mass Tethered System for Micro-*g*/Variable-*g* Applications," *Journal of Guidance, Control, and Dynamics,* Vol. 10, No. 3, 1987, pp. 242-249.

[13]Lorenzini, E. C., Cosmo, M., Vetrella, S., and Moccia, A., "Dynamics and Control of the Tether Elevator/Crawler System," *Journal of Guidance, Control, and Dynamics,* Vol. 12, No. 3, 1989, pp. 404-411.

[14]Bainum, P. M., and Kumar, V. K., "Optimal Control of the Shuttle-Tethered-Subsatellite System," *Acta Astronautica,* Vol. 7, No. 12, 1980, pp. 1333-1348.

[15]Fan, R., and Bainum, P. M., "Dynamics and Control of a Space Platform with a Tethered Subsatellite," *Journal of Guidance, Control, and Dynamics,* Vol. 11, No. 4, 1988, pp. 377-381.

[16]Moccia, A., and Vetrella, S., "Dynamics and Control of Two Space Platforms Connected by a Short Tether," *Space Tethers for Science in the Space Station Era,* Societa Italiana di Fisica, Conf. Proceedings, Vol. 14, Venice, Italy, Oct. 1987, pp. 104-110.

[17]Venditti, F., Cibario, B., and Musetti, B., "Dynamics Simulation of the TSS Actively Controlled Satellite," *Space Tethers for Science in the Space Station Era,* Societa Italiana di Fisica, Conf. Proceedings, Vol. 14, Venice Italy, Oct. 1987, pp. 116-129.

[18]Lemke, L. G., Powell, J. D., and He, X., "Attitude Control of Tethered Spacecraft," *Journal of the Astronautical Sciences,* Vol. 35, No. 1, 1987, pp. 41-55.

[19]Penzo, P., "VISTA (Vertical Interferometric SAR Tethered Altimeter) Tether Control System Concept," JPL/ASI Technical Meeting, Rome, Italy, April 1990.

[20]Vetrella, S., Moccia, A., Lorenzini, E. C., and Cosmo, M., "Attitude Dynamics of the Tether Elevator/Crawler System for Microgravity Applications," *ESA Journal,* Vol. 14, No. 3, 1990, pp. 303-312.

[21]Penzo, P. A., "An Earth Explorer Global Topography Mission," JPL/ASI Technical Meeting, Jet Propulsion Lab., Pasadena, CA, Feb. 1990.

[22]von Flotow, A. H., "Some Approximations for the Dynamics of Spacecraft Tethers," *Journal of Guidance, Control, and Dynamics,* Vol. 11, No. 4, 1988, pp. 357-364.

[23]Misra, A. K., and Modi, V. J., "A Survey on the Dynamics and Control of Tethered Satellite System," *American Astronautical Society (AAS) Advances in Astronautical Sciences,* Vol. 62, 1987, pp. 667-719.

[24]Graziani, F., Sgubini, S., and Agneni, A., "Disturbance Propagation in Orbiting Tethers," *American Astronautical Society (AAS) Advances in Astronautical Sciences,* Vol. 62, 1987, pp. 301-315.